Electronic Supplementary Material (ESI) for New Journal of Chemistry.
This journal is © The Royal Society of Chemistry and the Centre National de la Recherche Scientifique 2021

Electronic Supporting Information

Synthesis and triplet sensitization of bis(arylselanyl)BOPHY; potential application in triplet-triplet annihilation upconversion

Ryohei Hasegawa, Shinji Iwakiri and Yuji Kubo*

Department of Applied Chemistry, Graduate School of Urban Environmental Sciences, Tokyo Metropolitan University, 1-1 Minami-Osawa, Hachioji, Tokyo, 192-0397

Table of contents

Fig. S1. Absorption and fluorescence spectra of **1** in various solvent S-2
Table S1. Photophysical properties of **1** in various solvent S-2
Fig. S2. Absorption and fluorescence spectra of **2** in various solvent S-3
Table S2. Photophysical properties of **2** in various solvent S-3
Fig. S3. Absorption and fluorescence spectra of **3** in various solvent S-4
Table S3. Photophysical properties of **3** in various solvent S-4
Fig. S4. Absorption and fluorescence spectra of **I_2BOPHY** in various solvent S-5
Table S4. Photophysical properties of **I_2BOPHY** in various solvent S-5
Fig. S5 Lippert-Mataga plot for **1**, **2**, **3** and **I_2BOPHY**. S-5
Fig. S6 Solid emission spectra of **1, 2, 3** and **I_2BOPHY** S-6
Table S5. Calculated values for **1.** S-6
Fig. S7. The frontier molecular orbitals of the optimized structures of **1.** S-6
Table S6. Calculated values for **2.** S-7
Fig. S8. The frontier molecular orbitals of the optimized structures of **2.** S-7
Table S7. Calculated values for **3.** S-8
Fig. S9. The frontier molecular orbitals of the optimized structures of **3.** S-8
Table S8. Calculated values for **I_2BOPHY.** S-9
Fig. S10. The frontier molecular orbitals of the optimized structures of **I_2BOPHY** S-9
Fig. S11. Fitting absorption spectral change for photooxidation of DPBF using **1-3**, **I_2BOPHY** S-10
Fig. S12. UC emission intensity at 412 nm at different power intensities S-10
Fig. S13– Fig. S25 Spectral data of structure assignment of the dyes ..... S-11 − S-23
Single crystal X-ray diffraction study for **1** ..... S-24 − S-31

Lippert-Mataga plot

$$\Delta f = \frac{D-1}{2D+1} - \frac{n^2-1}{2n^2+1} \qquad \tilde{\nu}_{\mathrm{abs}} - \tilde{\nu}_{\mathrm{em}} = \Delta f \frac{2(\mu_{\mathrm{E}} - \mu_{\mathrm{G}})^2}{hcr^3} + const.$$

Δf is the orientational polarisability where D and n are dielectric constant and refractive index, respectively. The parameters of h, c, and r are the Plank's constant, the velocity of light, and the Onsager radius r, respectively. DFT calculation (B3LYP/6-31G(d,p)) was used to estimate r. A linear relationship between the Stokes shift ($\tilde{\nu}_{\mathrm{abs}} - \tilde{\nu}_{\mathrm{em}}$) and Δf was obtained (Figure S1) to afford the difference between excited- and ground-state dipole moments.

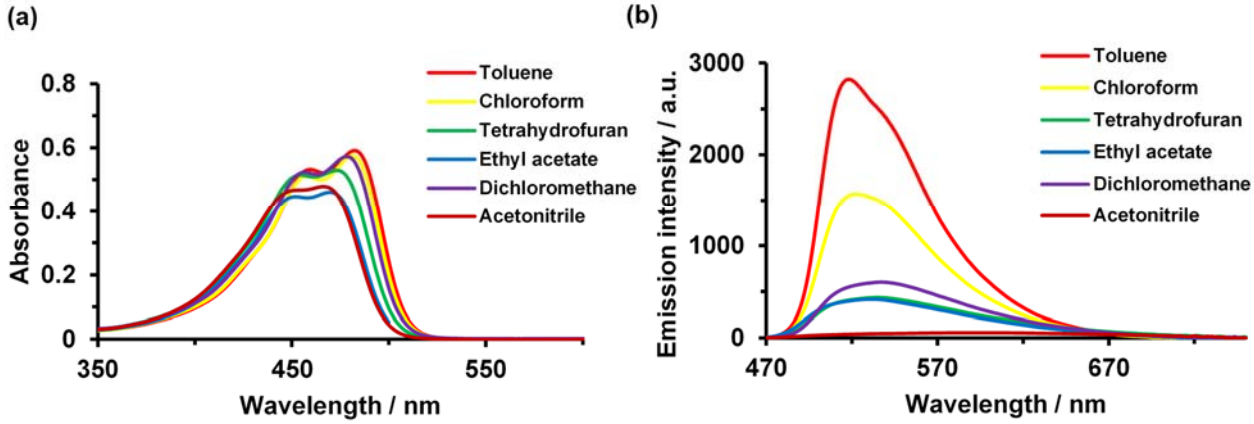

Fig. S1. Absorption (a) fluorescence spectra (b) of **1** in different solvent (10 μM), λ_{ex} = 460 nm, 25°C.

Table S1. Photophysical properties of **1** in different solvents.

Solvent	$\lambda_{abs}{}^{a}$ / nm	ε^{b} / $\times 10^4$ M^{-1} cm^{-1}	$\lambda_{em}{}^{c}$ / nm	$\Phi_F{}^{d}$ / %	$\Delta\nu$ ^{e} / cm^{-1}
Toluene	459 / 482	5.36 / 5.93	519	9.19	1479
Chloroform	457 / 481	5.40 / 6.10	526	5.02	1779
Tetrahydrofuran	454 / 473	5.50 / 5.66	534	2.09	2415
Ethyl acetate	452 / 470	5.67 / 5.87	534	2.00	2550
Dichloromethane	456 / 478	5.48 / 6.01	540	2.11	2402
Acetonitrile	454 / 466	5.48 / 5.62	598	0.359	4737

[a]Maximal absorption wavelength. [b]Molar extinction coefficient at 10^4 M^{-1} cm^{-1}. [c]Maximal fluorescence wavelength (λ_{ex} = 460 nm). [d] Fluorescence quantum yields.[e] $\Delta\nu = (1/\lambda_{abs}) - (1/\lambda_F)$. λ_{abs} and λ_F correspond to maximal absorption and maximal emission wavelengths, respectively.

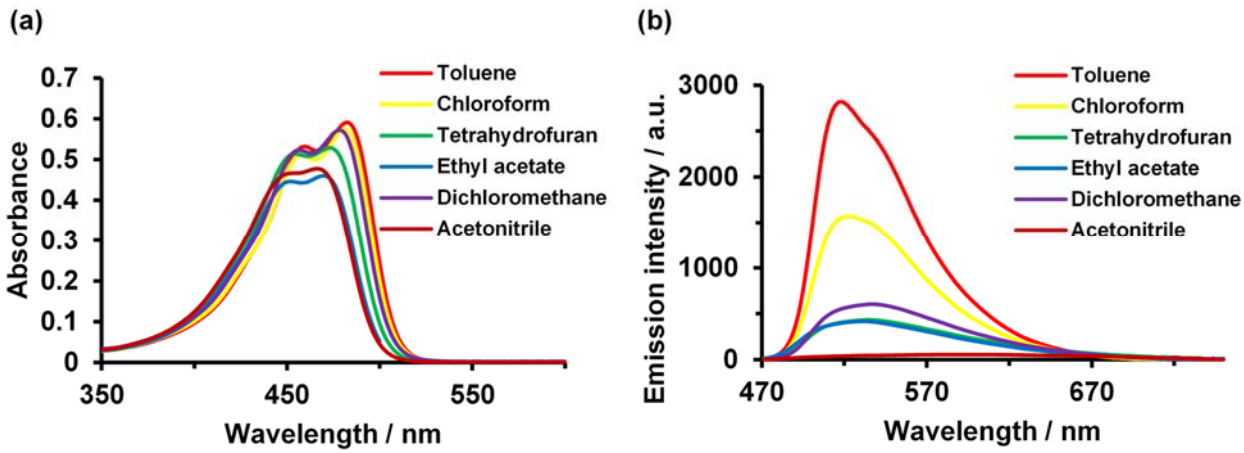

Fig. S2. Absorption (a) fluorescence spectra (b) of **2** in different solvent (10 μM), λ_{ex} = 460 nm, 25°C.

Table S2. Photophysical properties of **2** in different solvents.

Solvent	$\lambda_{abs}{}^{a}$ / nm	ε^{b} / $\times 10^4$ M^{-1} cm^{-1}	$\lambda_{em}{}^{c}$ / nm	$\Phi_F{}^{d}$ / %	$\Delta\nu^{e}$ / cm^{-1}
Toluene	459 / 482	5.32 / 5.91	517	8.95	1405
Chloroform	458 / 481	5.11 / 5.75	522	5.36	1633
Tetrahydrofuran	454 / 473	5.14 / 5.29	534	1.90	2415
Ethyl acetate	454 / 470	4.45 / 4.60	533	2.00	2515
Dichloromethane	457 / 478	5.23 / 5.72	537	2.43	2299
Acetonitrile	453 / 466	4.67 / 4.78	586	0.380	4394

[a]Maximal absorption wavelength. [b]Molar extinction coefficient at 10^4 M^{-1} cm^{-1}. [c]Maximal fluorescence wavelength (λ_{ex} = 460 nm). [d]Fluorescence quantum yields. [e]$\Delta\nu = (1/\lambda_{abs}) - (1/\lambda_F)$. λ_{abs} and λ_F correspond to the maximal absorption and maximal emission wavelengths, respectively.

.

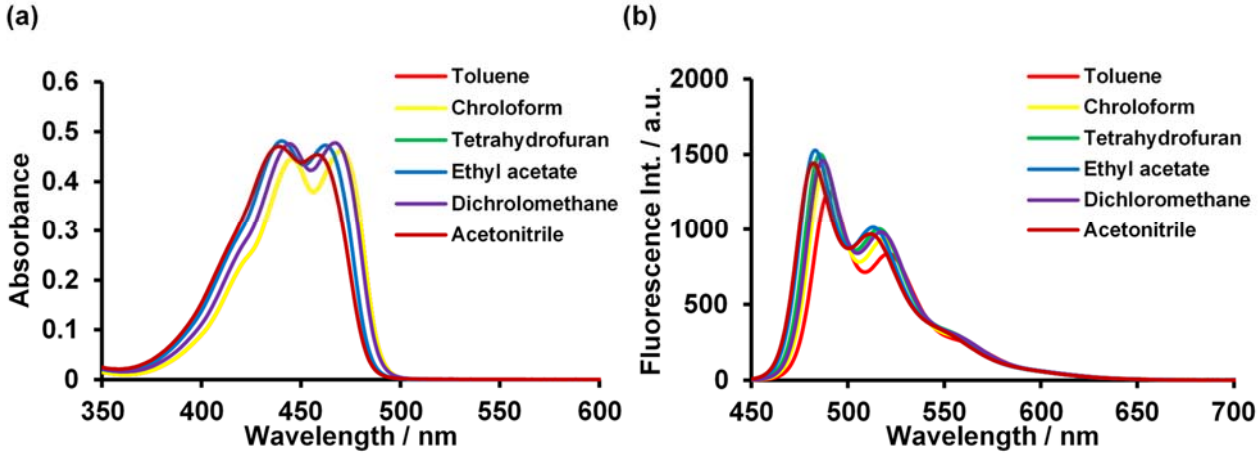

Fig. S3. Absorption (a) fluorescence spectra (b) of **3** in different solvent (10 μM), λ_{ex} = 440 nm, 25°C.

Table S3. Photophysical properties of **3** in different solvents.

Solvent	$\lambda_{abs}{}^{a}$ / nm	ε^{b} / $\times 10^4$ M^{-1} cm^{-1}	$\lambda_{em}{}^{c}$ / nm	$\Phi_F{}^{d}$ / %	$\Delta\nu$ ^{e} / cm^{-1}
Toluene	447 / 471	4.52 / 4.69	490 / 521	96.6	823
Chloroform	445 / 470	4.45 / 4.62	488 / 518	96.6	785
Tetrahydrofuran	443 / 465	4.69 / 4.61	485 / 516	89.7	887
Ethyl acetate	440 / 462	4.81 / 4.73	483 / 513	82.6	941
Dichloromethane	444 / 467	4.75 / 4.77	487 / 517	89.8	879
Acetonitrile	438 / 458	4.70 / 4.54	482 / 511	79.7	1087

[a]Maximal absorption wavelength. [b] Molar extinction coefficient at 10^4 M^{-1} cm^{-1}. [c]Maximal fluorescence wavelength (λ_{ex} = 440 nm). [d]Fluorescence quantum yields. [e]$\Delta\nu = (1/\lambda_{abs}) - (1/\lambda_F)$. λ_{abs} and λ_F correspond to maximum absorption and maximum emission wavelengths, respectively.

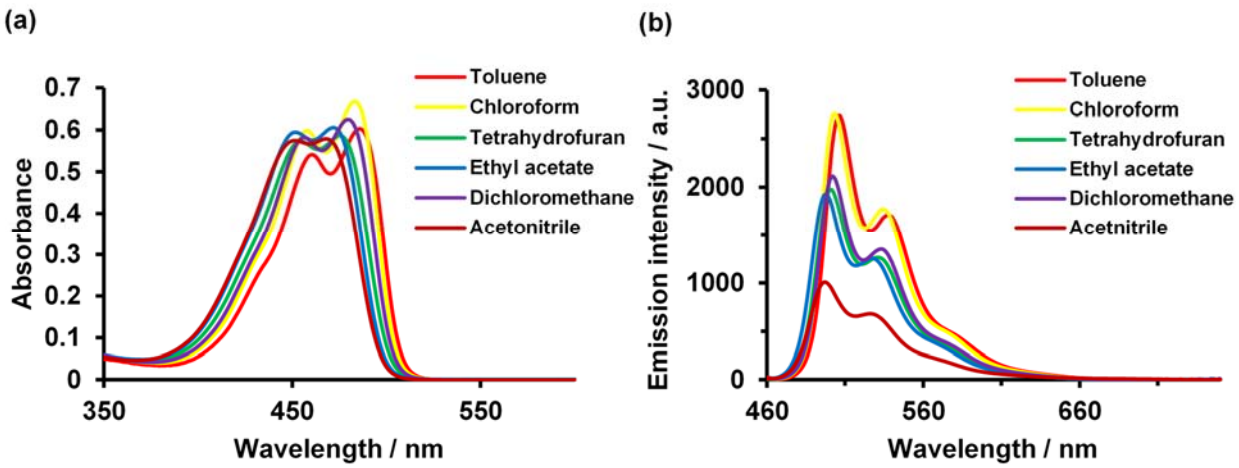

Fig. S4. Absorption (a) fluorescence spectra (b) of **I_2BOPHY** in different solvent (10 μM), λ_{ex} = 460 nm, 25°C.

Table S4. Photophysical properties of **I_2BOPHY** in different solvents.

Solvent	$\lambda_{abs}{}^{a}$ / nm	ε^{b} / $\times 10^4$ M^{-1} cm^{-1}	$\lambda_{em}{}^{c}$ / nm	$\Phi_F{}^{d}$ / %	$\Delta\nu^{e}$ / cm^{-1}
Toluene	460 / 486	5.41 / 6.03	506 / 537	24.1	777
Chloroform	458 / 484	5.99 / 6.67	503 / 534	19.6	780
Tetrahydrofuran	455/ 476	5.73 / 5.87	501 / 531	14.7	1048
Ethyl acetate	452 / 472	5.94 / 6.05	497 / 527	13.4	1066
Dichloromethane	457 / 480	5.82 / 6.25	502 / 533	15.4	913
Acetonitrile	452 / 468	5.75 / 5.79	497 / 526	7.31	1247

[a]Maximal absorption wavelength. [b]Molar extinction coefficient at 10^4 M^{-1} cm^{-1}. [c]Maximal fluorescence wavelength (λ_{ex} = 460 nm). [d]Fluorescence quantum yields. [e]$\Delta\nu = (1/\lambda_{abs}) - (1/\lambda_F)$. λ_{abs} and λ_F correspond to the maximal absorption and maximal emission wavelengths, respectively.

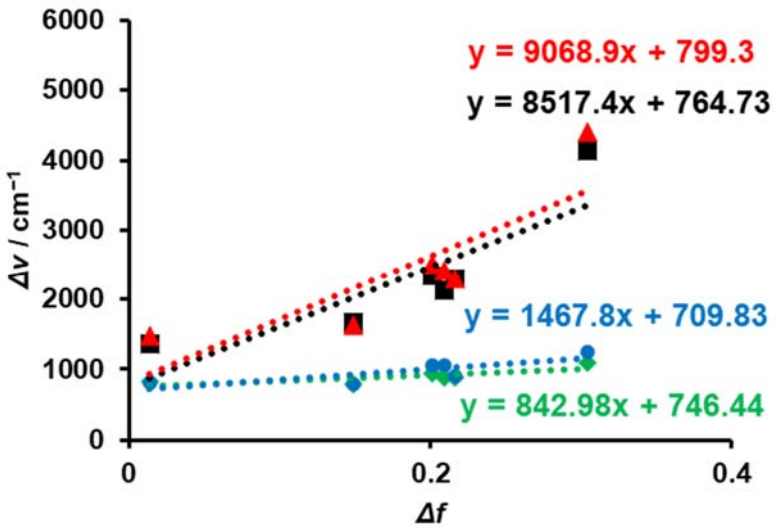

Fig. S5. Lippert-Mataga plot for for **1** (■), **2** (▲), **3** (◆) and **I_2BOPHY** (●) .

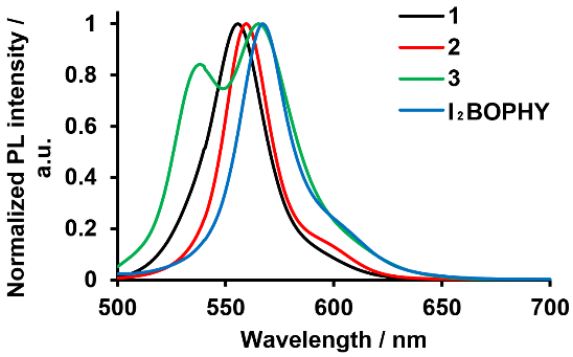

Fig. S6. Fluorescence spectra of **1**, **2**, **3** and **I$_2$BOPHY** in the solid state. λ_{ex} = 440 nm for **3**. λ_{ex} = 460 nm for **1**, **2** and **I$_2$BOPHY**, 25 °C.

Table S5. Calculated values of excited wavelength (λ_{calcd}), oscillator strength (f) and molecular orbital (MO) transition assignment for selected transition energies for **1**.

State	$\lambda_{(calcd.)}$ / nm	E / eV	$f_{(calcd.)}$	Calculated assignment [a]
$S_0 \rightarrow S_1$	468.8	2.64	0.2555	HOMO−2 → LUMO (2.7%)
				HOMO → LUMO (95.9%)
$S_0 \rightarrow S_2$	460.9	2.69	0.0026	HOMO−1 → LUMO (98.2%)
$S_0 \rightarrow S_3$	418.0	2.97	0.9713	HOMO−2 → LUMO (96.4%)
				HOMO → LUMO (2.8%)
$S_0 \rightarrow S_4$	339.4	3.65	0.0002	HOMO−3 → LUMO (70.3%)
				HOMO−2 → LUMO+1 (4.7%)
				HOMO → LUMO+1 (21.0%)

[a]Data given in parentheses are 2 × (CI coefficient)^2 × 100%; see the reference: M. Asgari, H. R. Memarian and H. Sabzyan, *J. Mol. Struct.*, 2020, **1207**, 127820.

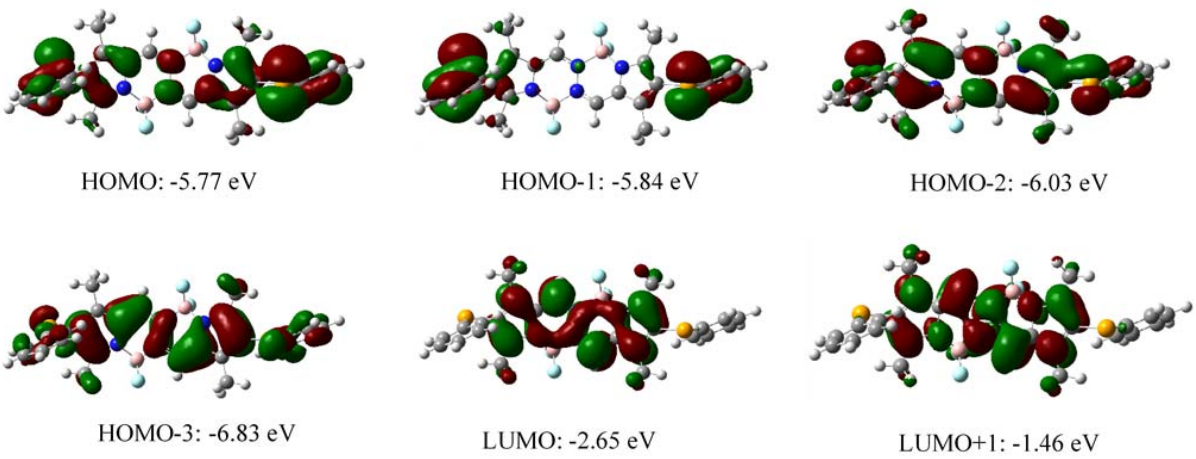

Fig. S7. The frontier molecular orbitals of the optimized structures of **1**.

Table S6. Calculated values of excited wavelength (λ_{calcd}), oscillator strength (f) and molecular orbital (MO) transition assignment for selected transition energies for **2**.

State	$\lambda_{(calcd.)}$ / nm	E / eV	$f_{(calcd.)}$	Calculated assignment [a]
$S_0 \rightarrow S_1$	455.0	2.73	0.4278	HOMO−2 → LUMO (4.0%)
				HOMO → LUMO (94.1%)
$S_0 \rightarrow S_2$	440.6	2.81	0.0384	HOMO−1 → LUMO (96.2%)
$S_0 \rightarrow S_3$	412.8	3.00	0.7551	HOMO−2 → LUMO (93.0%)
				HOMO → LUMO (4.6%)
$S_0 \rightarrow S_4$	337.5	3.67	0.0001	HOMO−3 → LUMO (70.0%)
				HOMO−2 → LUMO+1 (25.2%)

[a]Data given in parentheses are 2 × (CI coefficient)^2 × 100%; see the reference: M. Asgari, H. R. Memarian and H. Sabzyan, *J. Mol. Struct.*, 2020, **1207**, 127820.

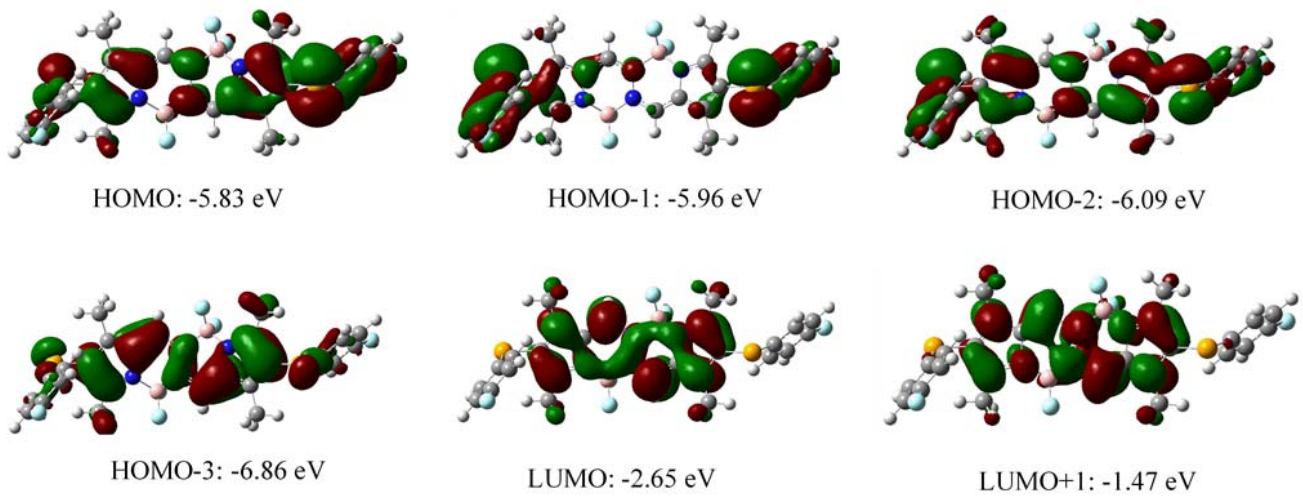

Fig. S8. The frontier molecular orbitals of the optimized structures of **2**.

Table S7. Calculated values of excited wavelength (λ_{calcd}), oscillator strength (f) and molecular orbital (MO) transition assignment for selected transition energies for **3**.

State	$\lambda_{(calcd.)}$ / nm	E / eV	$f_{(calcd.)}$	Calculated assignment [a]
$S_0 \rightarrow S_1$	417.0	2.97	0.9089	HOMO → LUMO (100%)
$S_0 \rightarrow S_2$	335.4	3.70	0.0000	HOMO−2 → LUMO (3.84%)
				HOMO−1 → LUMO (75.7%)
				HOMO → LUMO+1 (2.50%)
$S_0 \rightarrow S_3$	322.0	3.85	0.0013	HOMO−2 → LUMO (84.6%)
				HOMO → LUMO+1 (14.8%)
$S_0 \rightarrow S_4$	319.3	3.88	0.0694	HOMO−3 → LUMO (99.0%)

[a]Data given in parentheses are 2 × (CI coefficient)^2 × 100%; see the reference: M. Asgari, H. R. Memarian and H. Sabzyan, J. Mol. Struct., 2020, 1207, 127820.

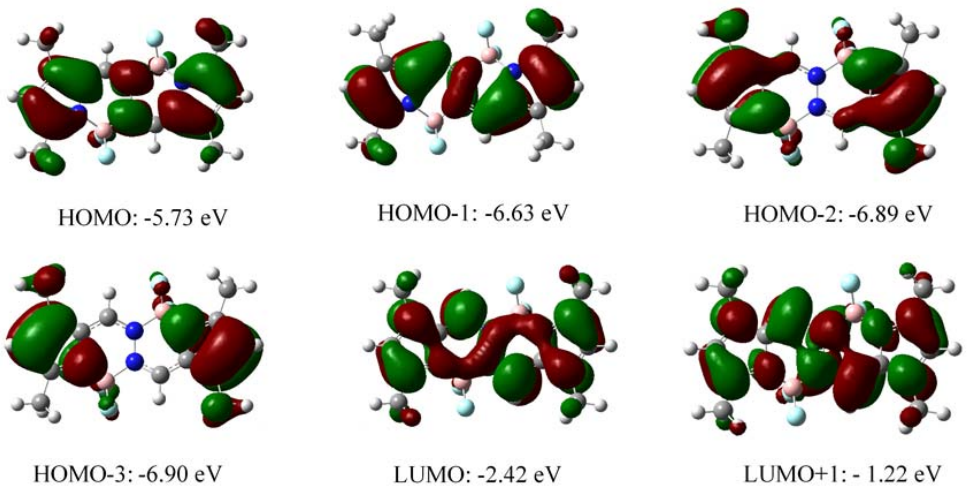

Fig. S9. The frontier molecular orbitals of the optimized structures of **3**.

Table S8. Calculated values of excited wavelength (λ_{calcd}), oscillator strength (f) and molecular orbital (MO) transition assignment for selected transition energies for **I_2-BOPHY**.

State	$\lambda_{(calcd.)}$ / nm	E / eV	$f_{(calcd.)}$	Calculated assignment [a]
$S_0 \rightarrow S_1$	409.0	3.03	0.8409	HOMO → LUMO (98.2%)
$S_0 \rightarrow S_2$	371.0	3.34	0.0001	HOMO−1 → LUMO (95.3%) HOMO → LUMO+1 (2.09%)
$S_0 \rightarrow S_3$	345.0	3.59	0.1732	HOMO−2 → LUMO (97.3%)
$S_0 \rightarrow S_4$	321.3	3.86	0.0000	HOMO−3 → LUMO (58.7%) HOMO → LUMO+1 (40.9%)

[a]Data given in parentheses are 2 × (CI coefficient)^2 × 100%; see the reference: M. Asgari, H. R. Memarian and H. Sabzyan, *J. Mol. Struct.*, 2020, **1207**, 127820.

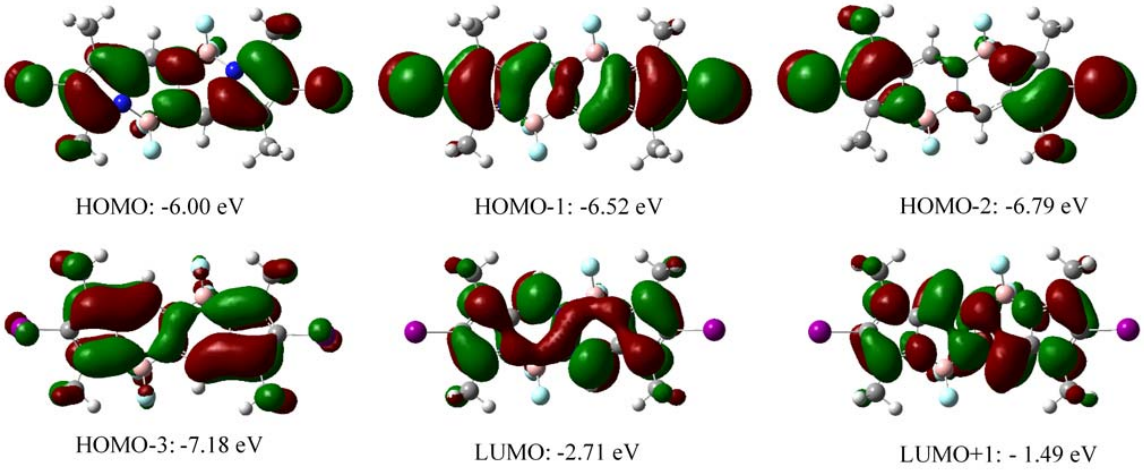

Fig. S10. The frontier molecular orbitals of the optimized structures of **I_2BOPHY**.

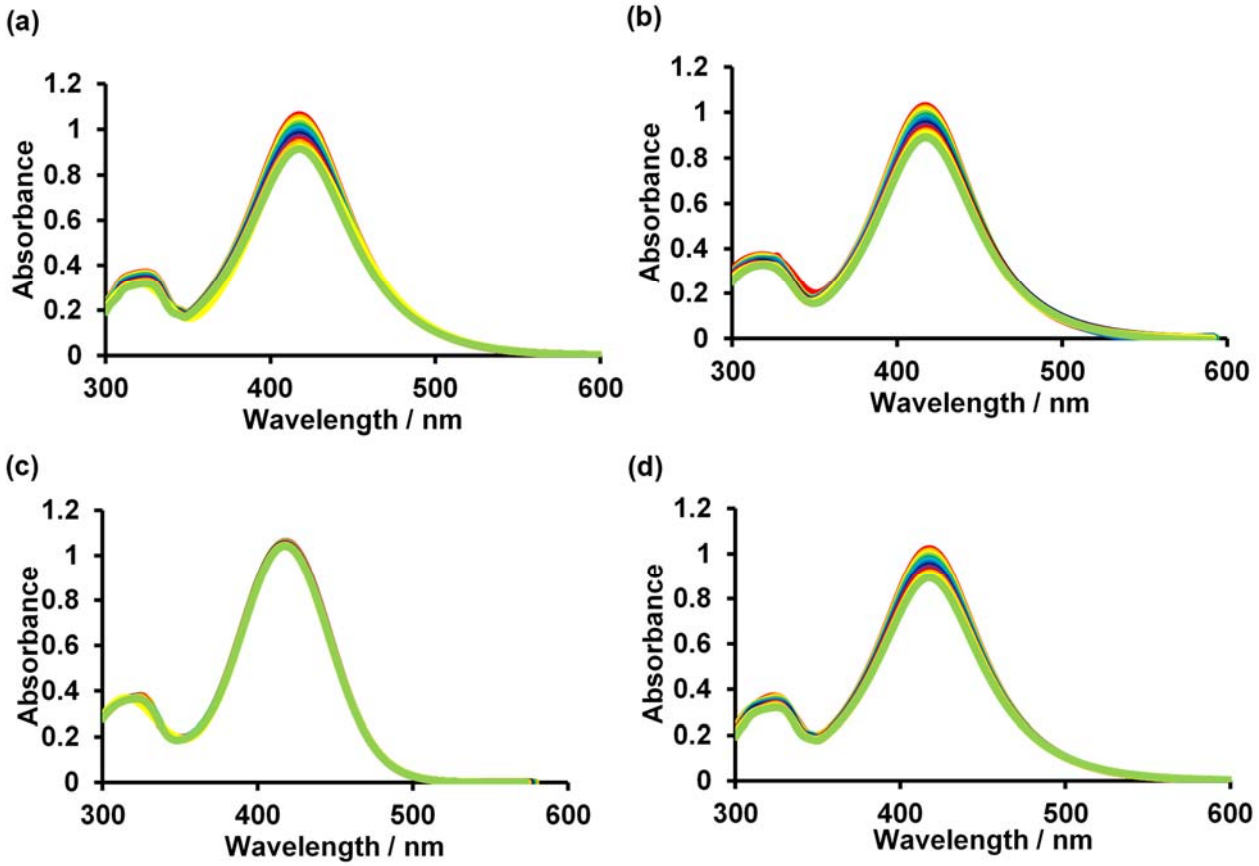

Fig. S11. Fitting absorption spectral change for photooxidation of DPBF (40 μM) using (a) **1**, (b) **2** (c) **3**, (d) **I_2BOPHY** as a photosensitizer.

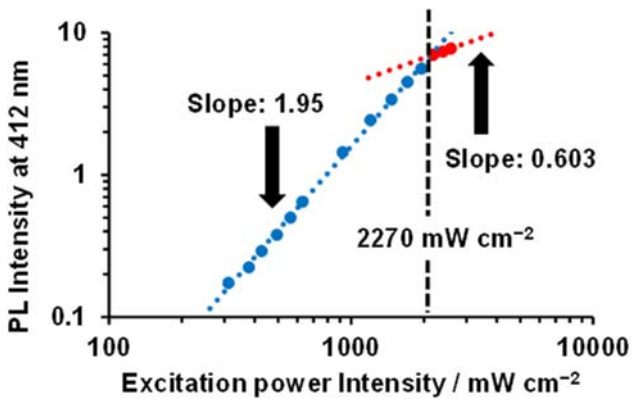

Fig. S12. UC emission intensity at 412 nm at different power intensities. [**1**] = 10 μM, [perylene] = 30 μM in deaerated toluene upon irradiation with a 524 nm laser (310 ~ 2600 mW cm^{-2}).

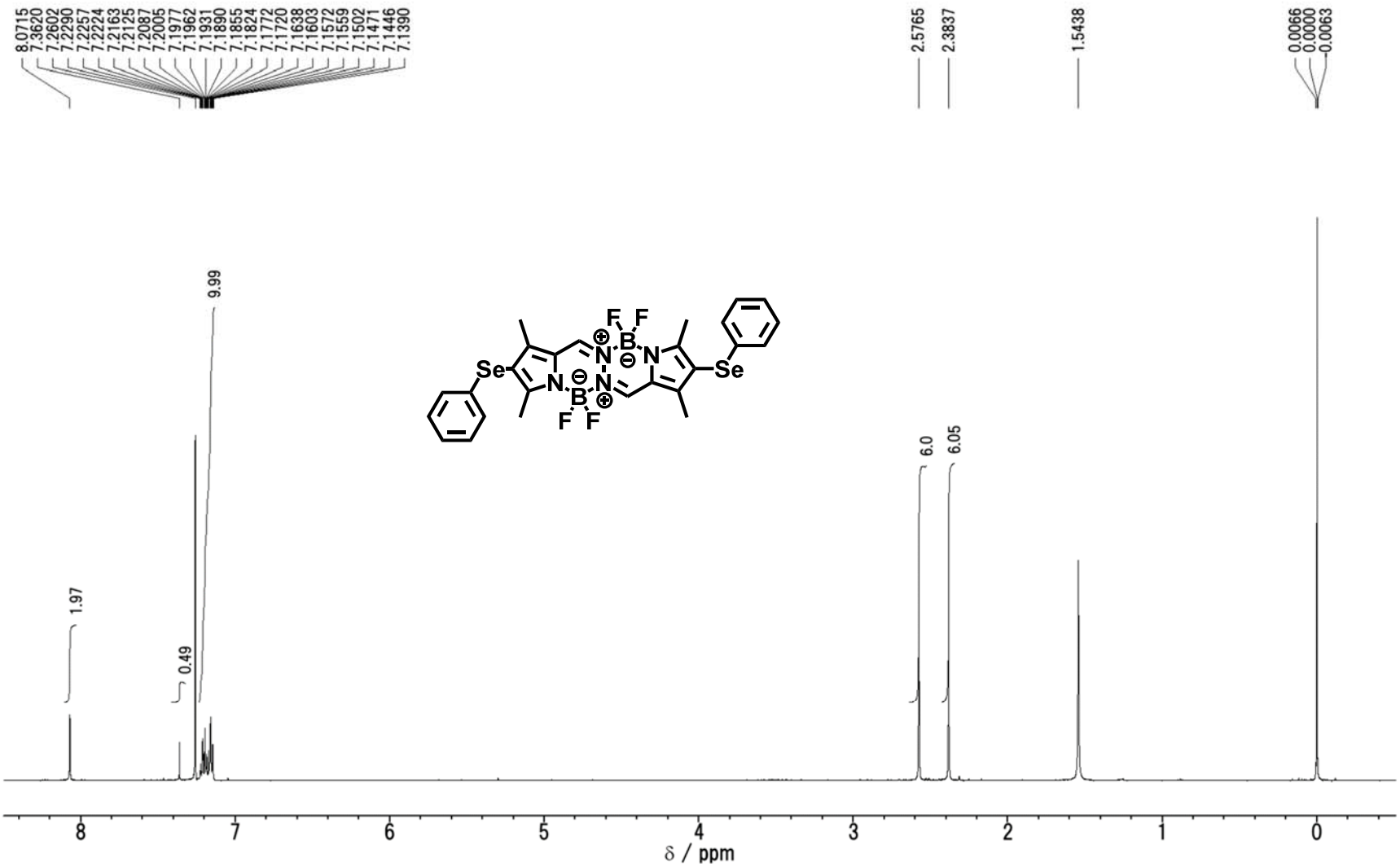

Fig. S13. ^{1}H NMR spectrum of **1** (500 MHz) in $CDCl_3$.

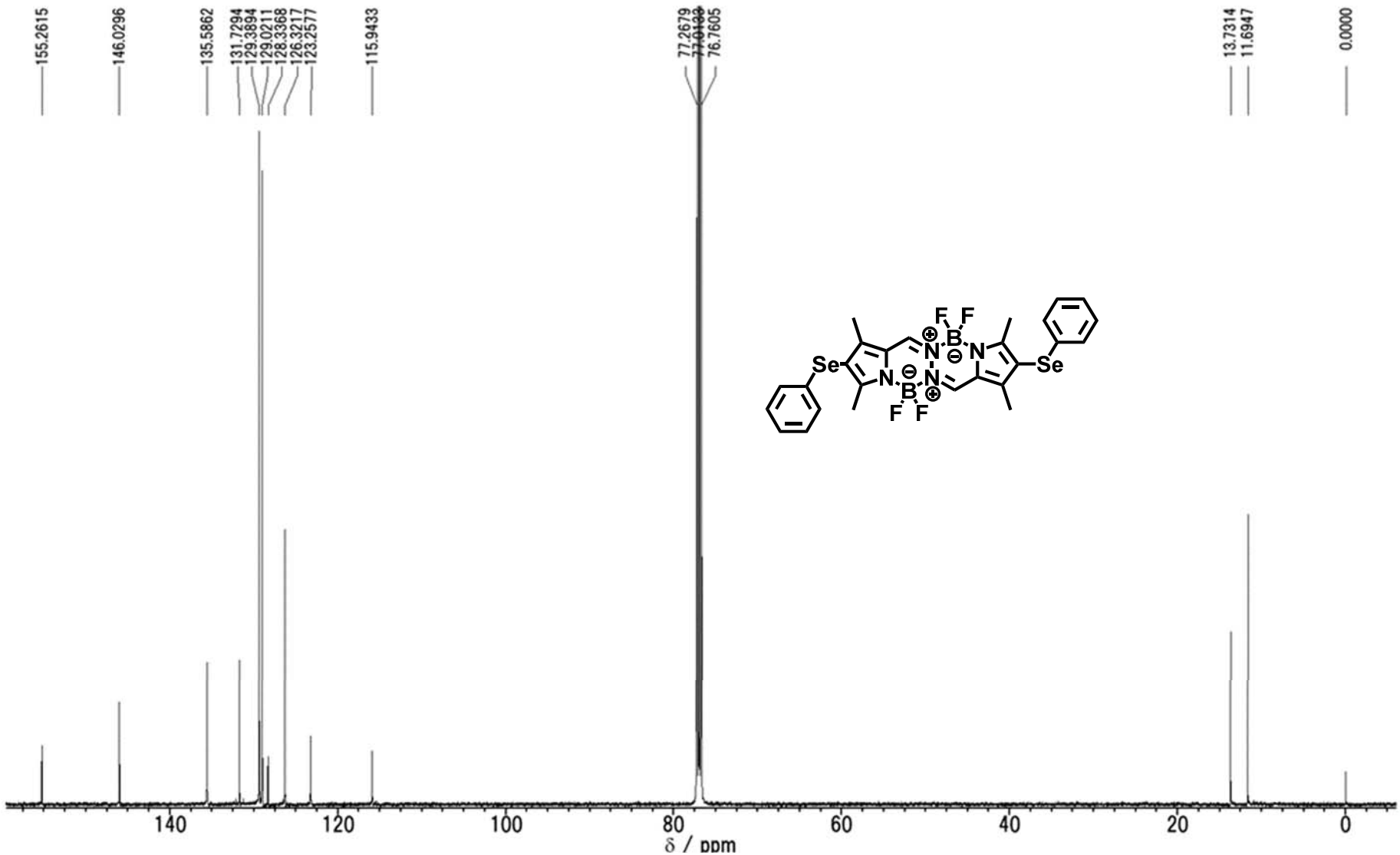

Fig. S14. ^{13}C NMR spectrum of **1** (126 MHz) in $CDCl_3$.

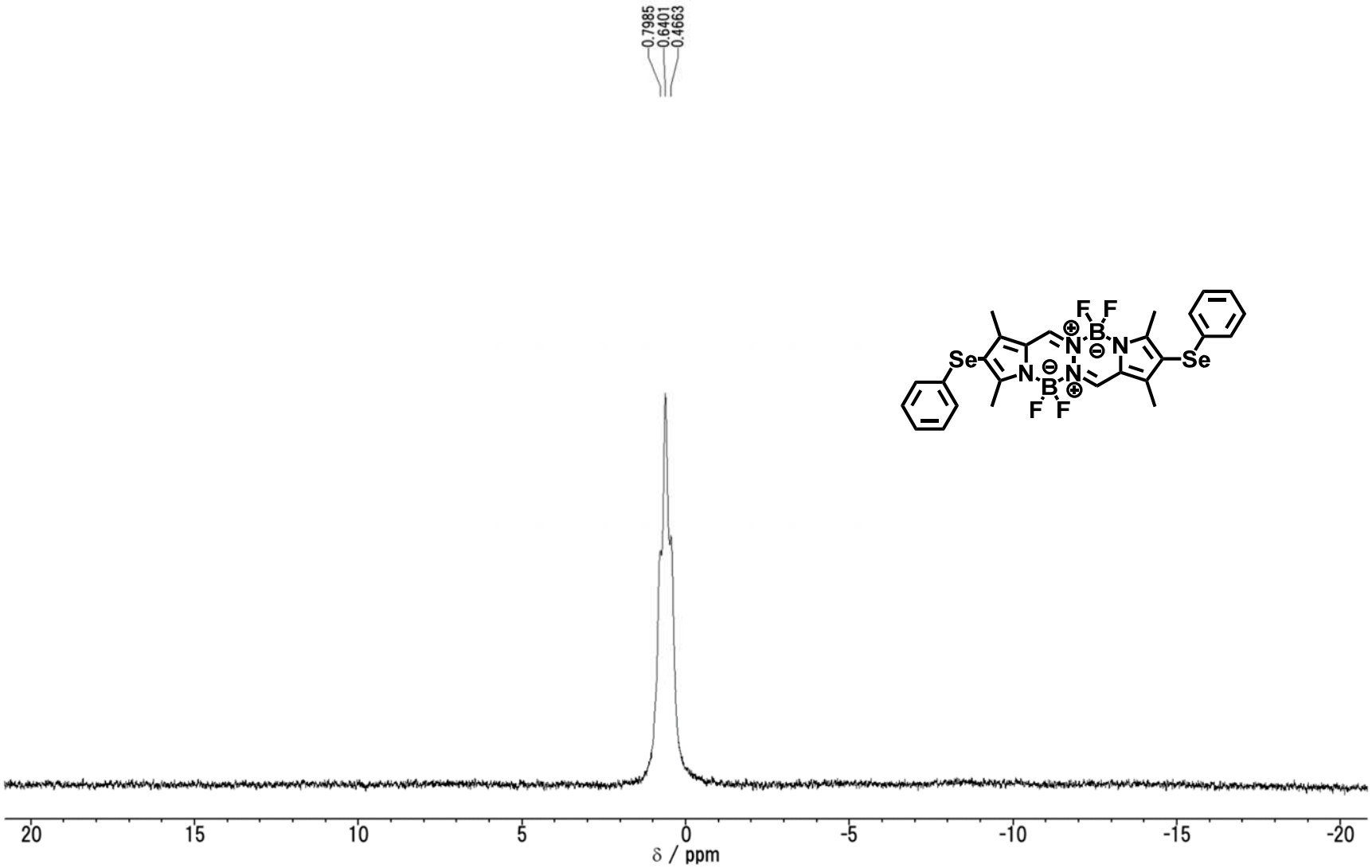

Fig. S15. ^{11}B NMR spectrum of **1** (160 MHz) in $CDCl_3$.

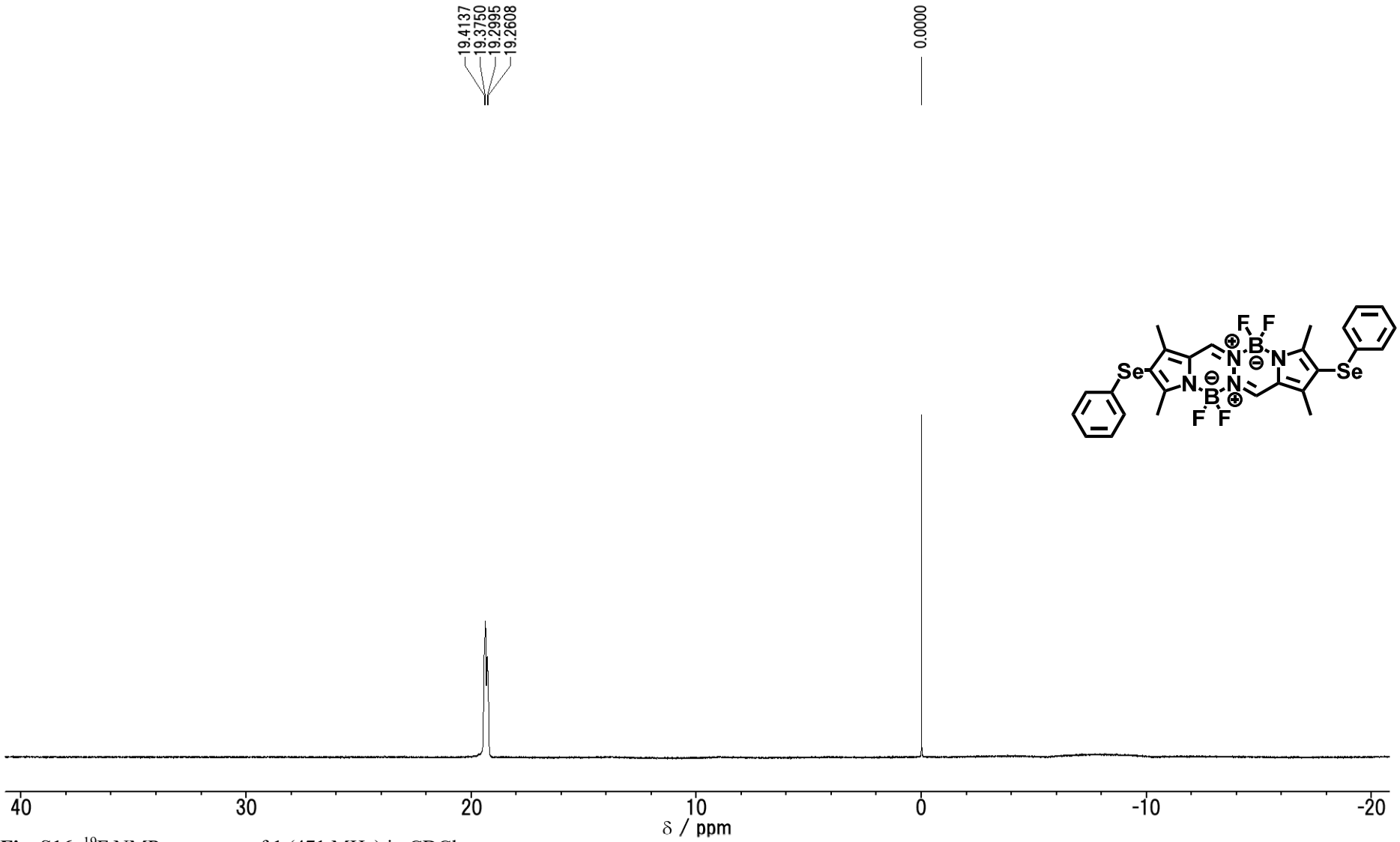

Fig. S16. ^{19}F NMR spectrum of **1** (471 MHz) in $CDCl_3$.

Generic Display Report

Analysis Info

Analysis Name	D:\Data\syn1\kubo20201219\#19_SeBPH_1.d	Acquisition Date	12/20/2020 5:16:30 AM
Method	APCI_pos_DIP.m	Operator	BDAL@DE
Sample Name	#19_SeBPH_1	Instrument	micrOTOF
Comment	Cap 150 Hex 400		

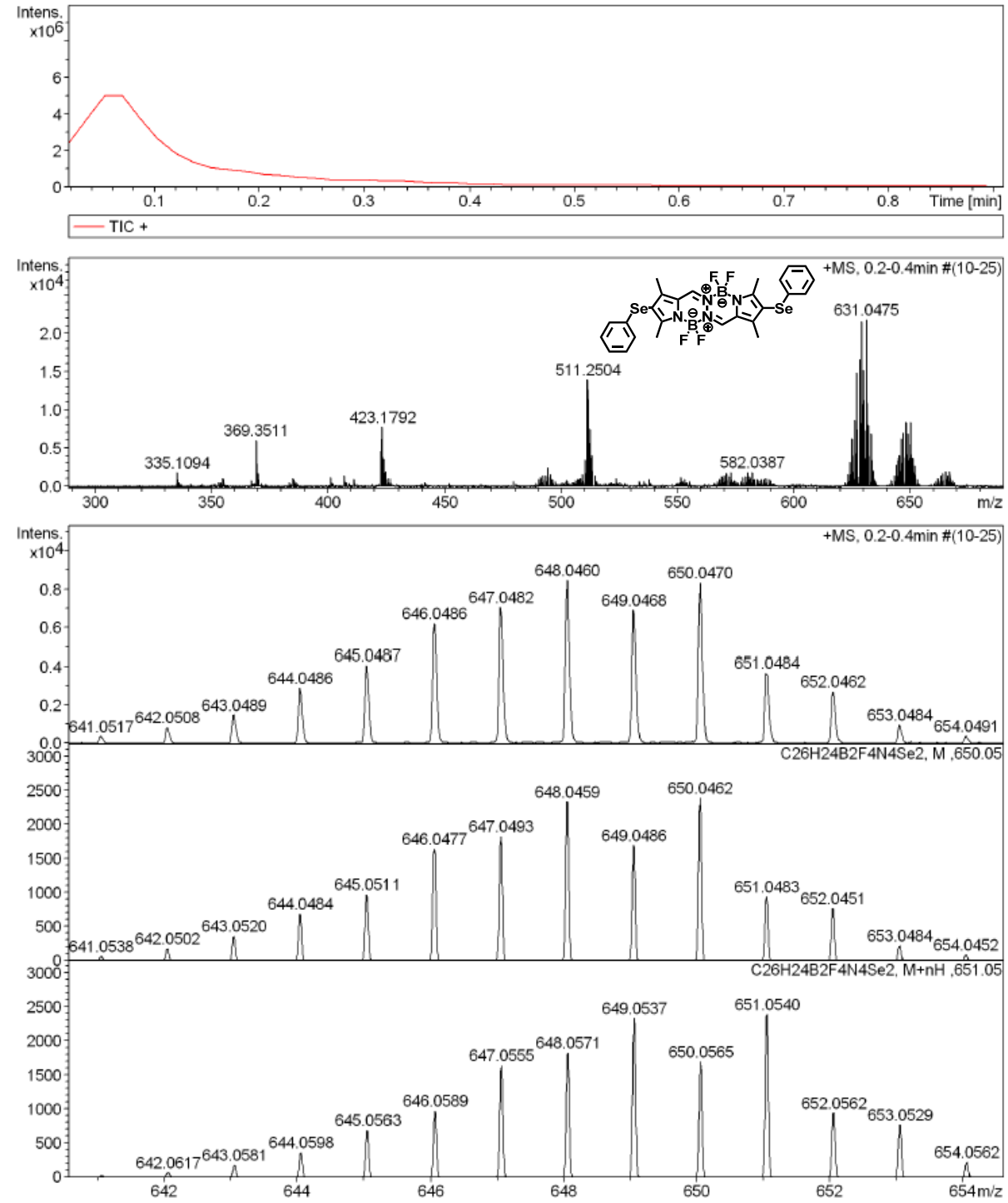

Bruker Compass DataAnalysis 4.0 printed: 12/19/2020 8:24:51 PM Page 1 of 1

Fig. S17. APCI mass spectrum of **1**.

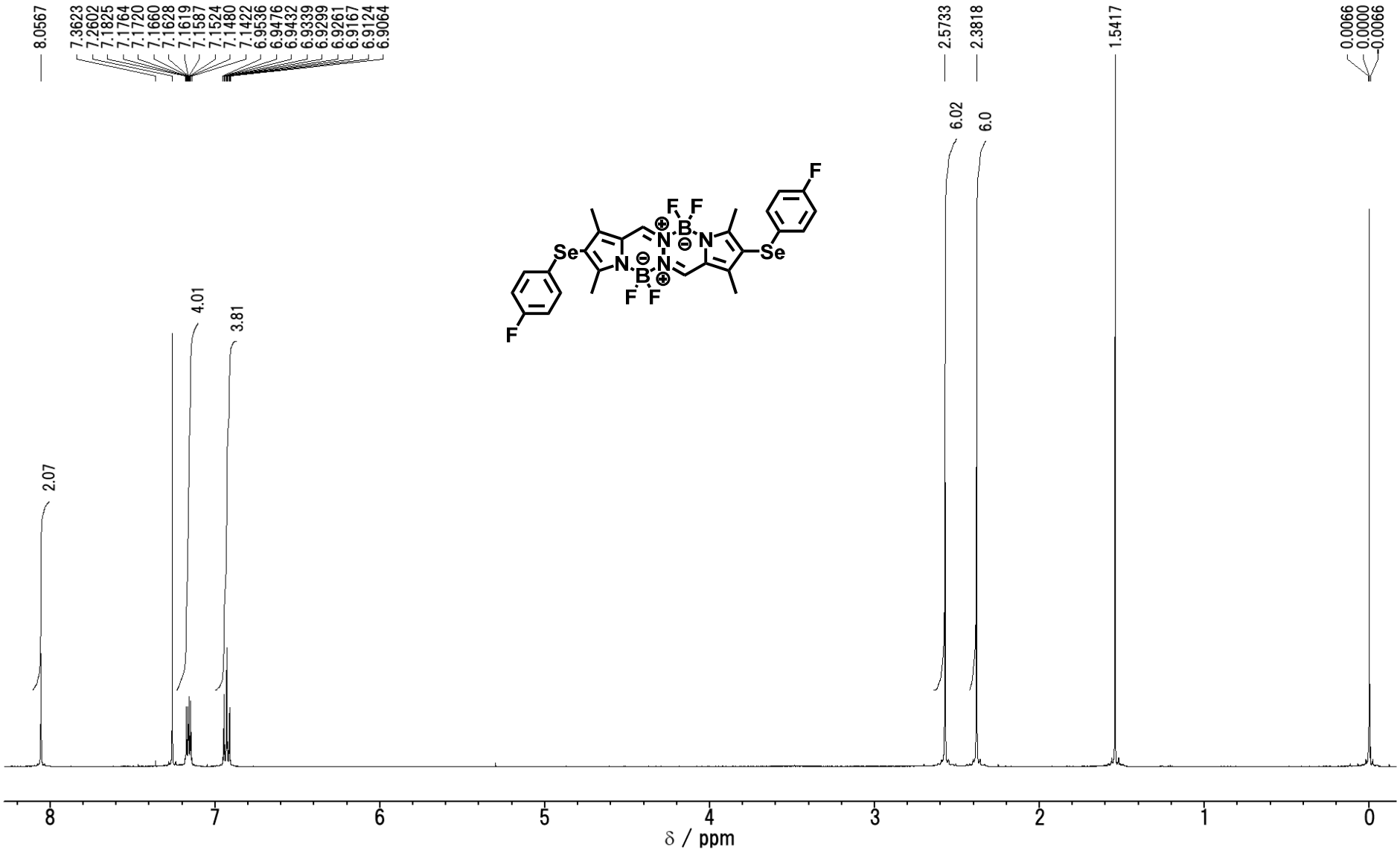

Fig. S18. ^{1}H NMR spectrum of **2** (500 MHz) in $CDCl_3$.

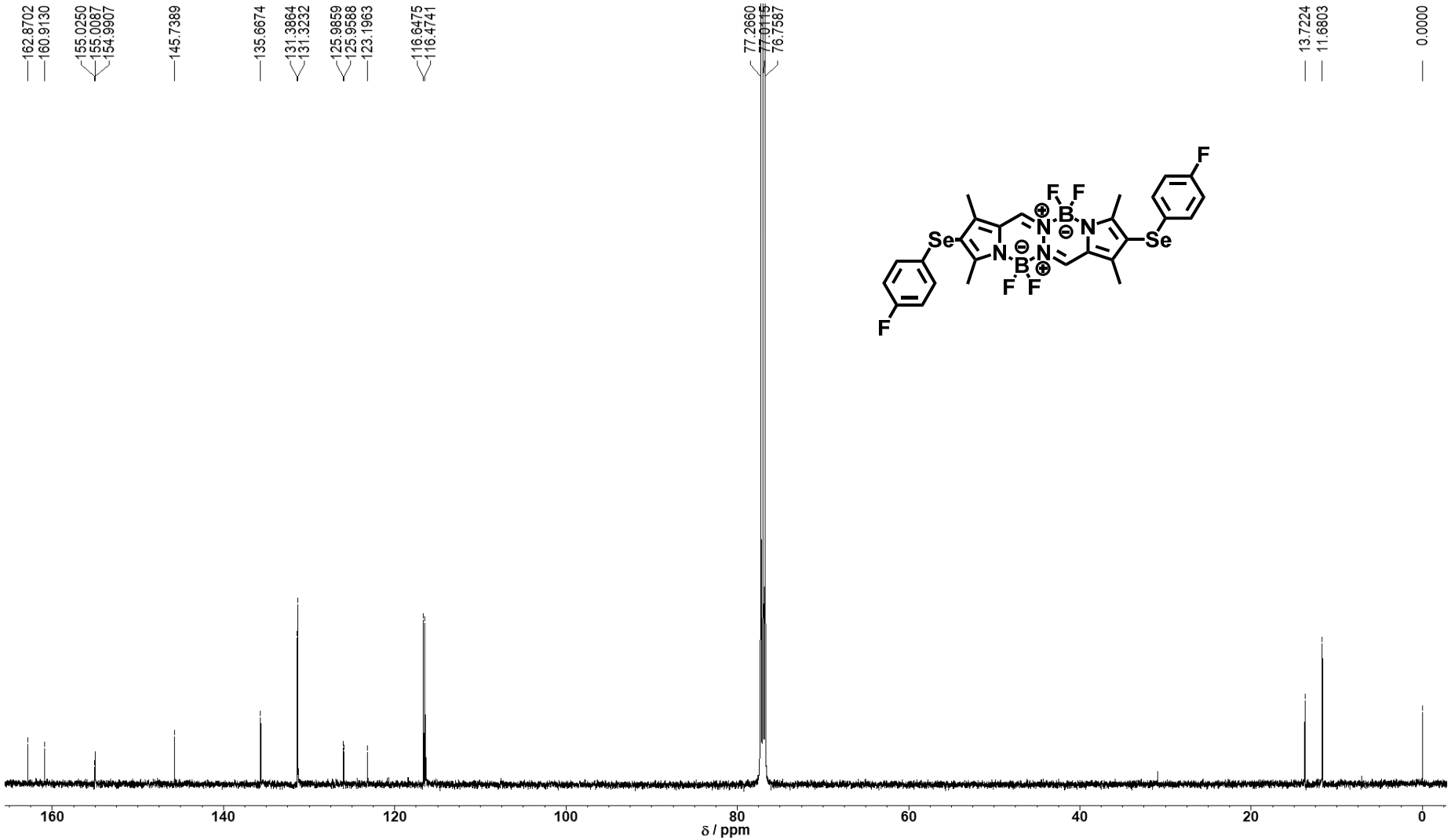

Fig. S19. ^{13}C NMR spectrum of **2** (126 MHz) in $CDCl_3$.

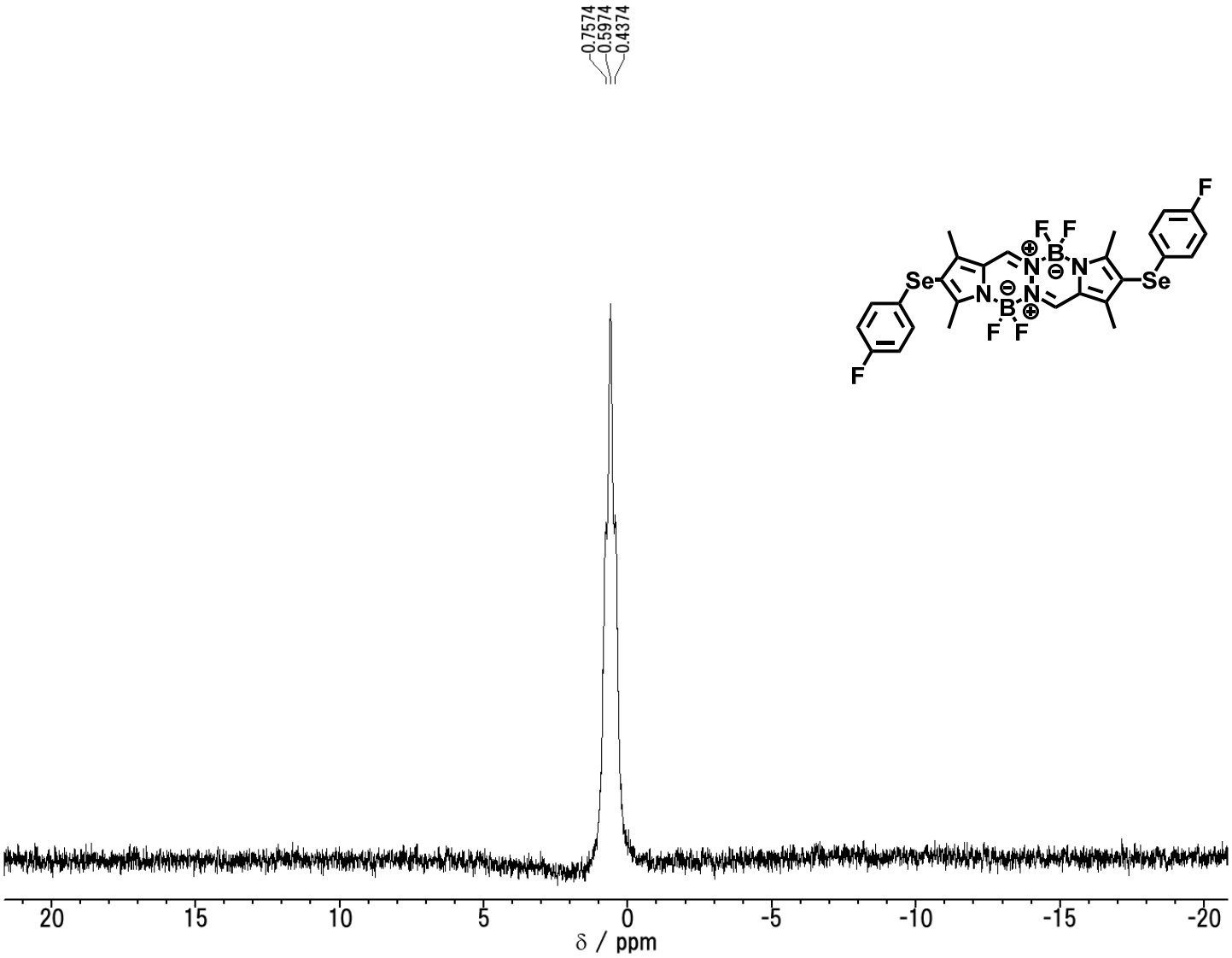

Fig. S20. ^{11}B NMR spectrum of **2** (160 MHz) in $CDCl_3$.

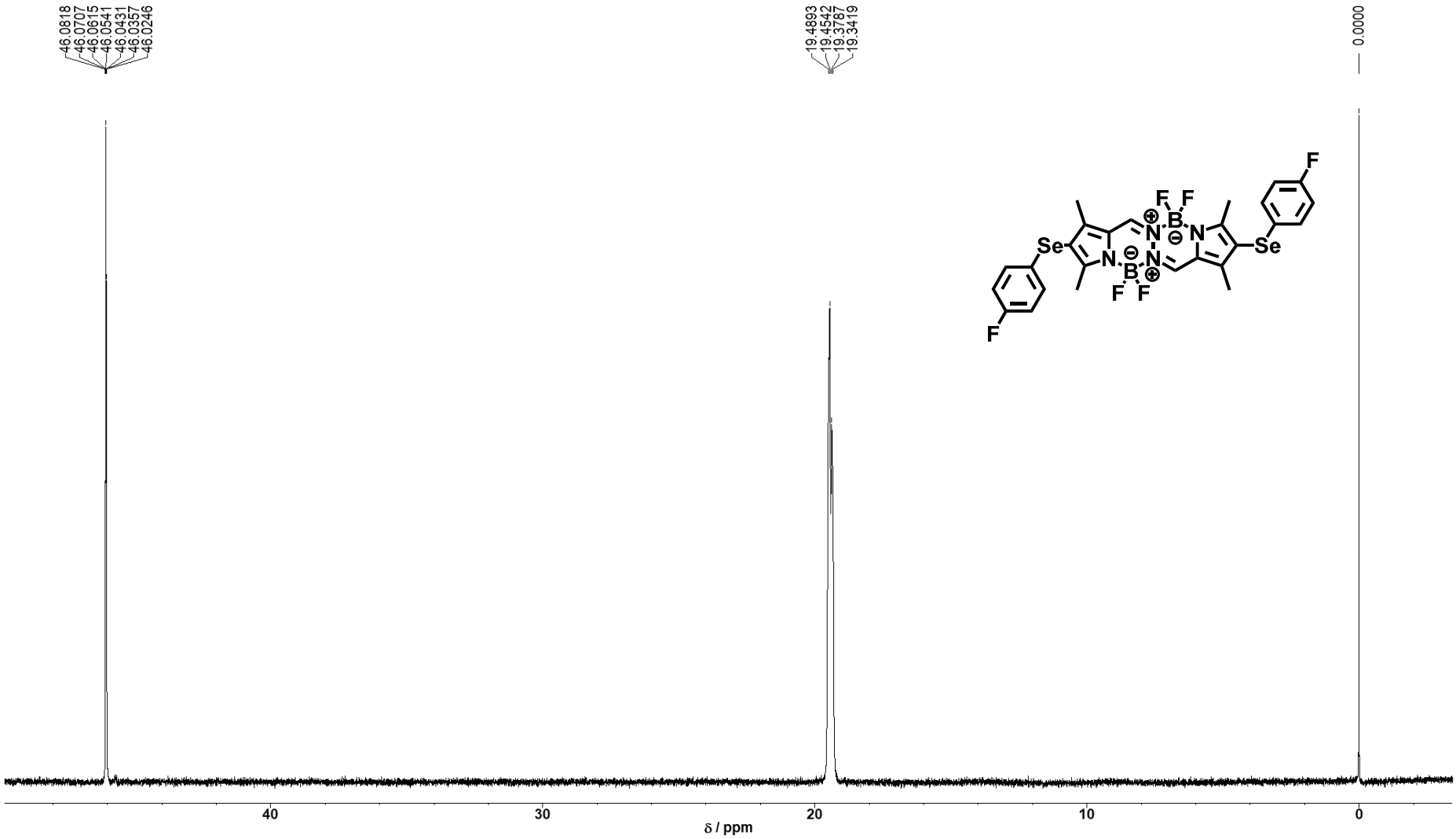

Fig. S21. ^{19}F NMR spectrum of **2** (471 MHz) in $CDCl_3$.

Generic Display Report

Analysis Info

Analysis Name	D:\Data\syn1\kubo20201219\#20_FSeBPH_1.d	Acquisition Date	12/20/2020 5:27:25 AM
Method	APCI_pos_DIP.m	Operator	BDAL@DE
Sample Name	#20_FSeBPH_1	Instrument	micrOTOF
Comment	Cap 150 Hex 400		

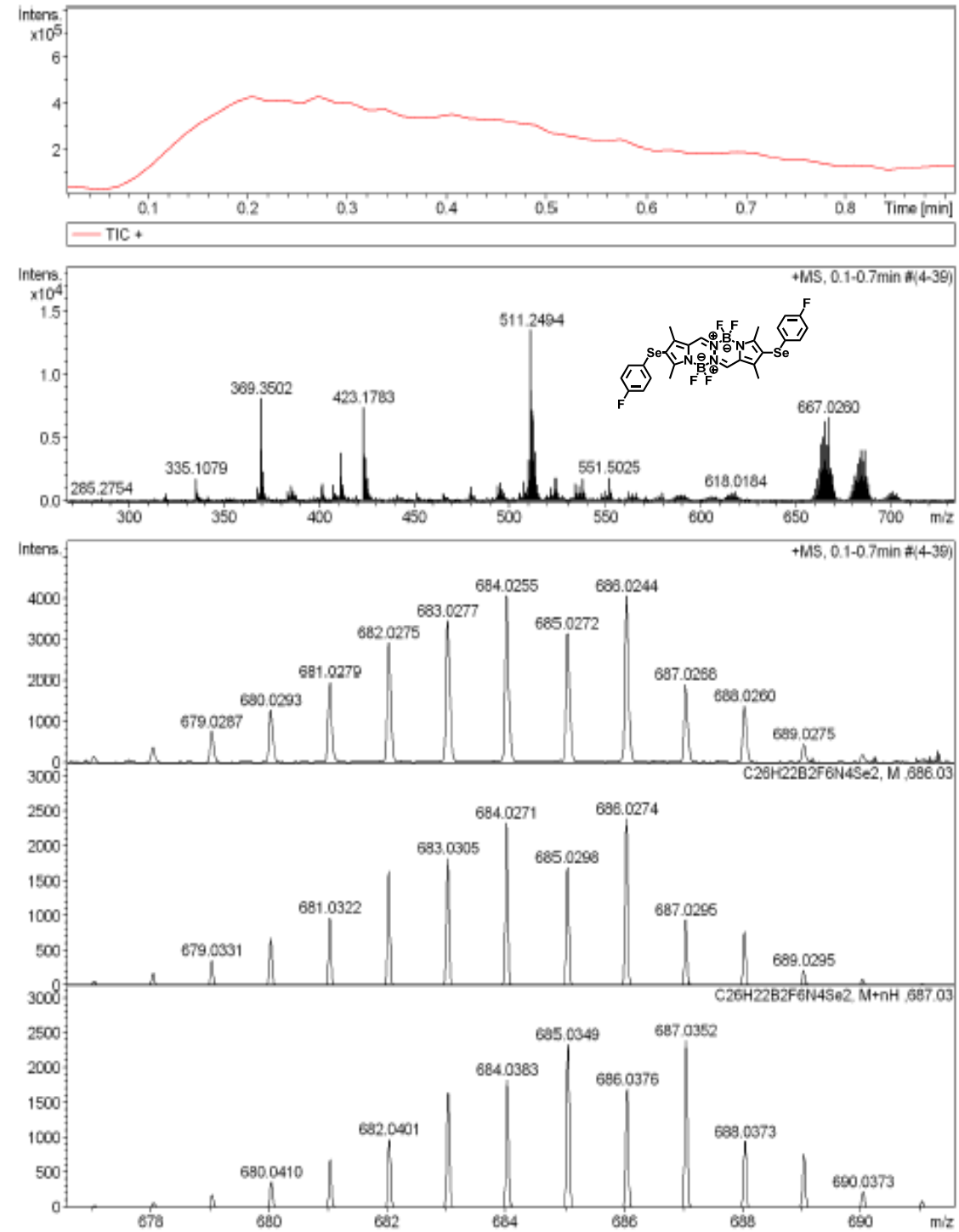

Bruker Compass DataAnalysis 4.0 printed: 12/19/2020 8:33:28 PM Page 1 of 1

Fig. S22. APCIPCI mass spectrum of **2**.

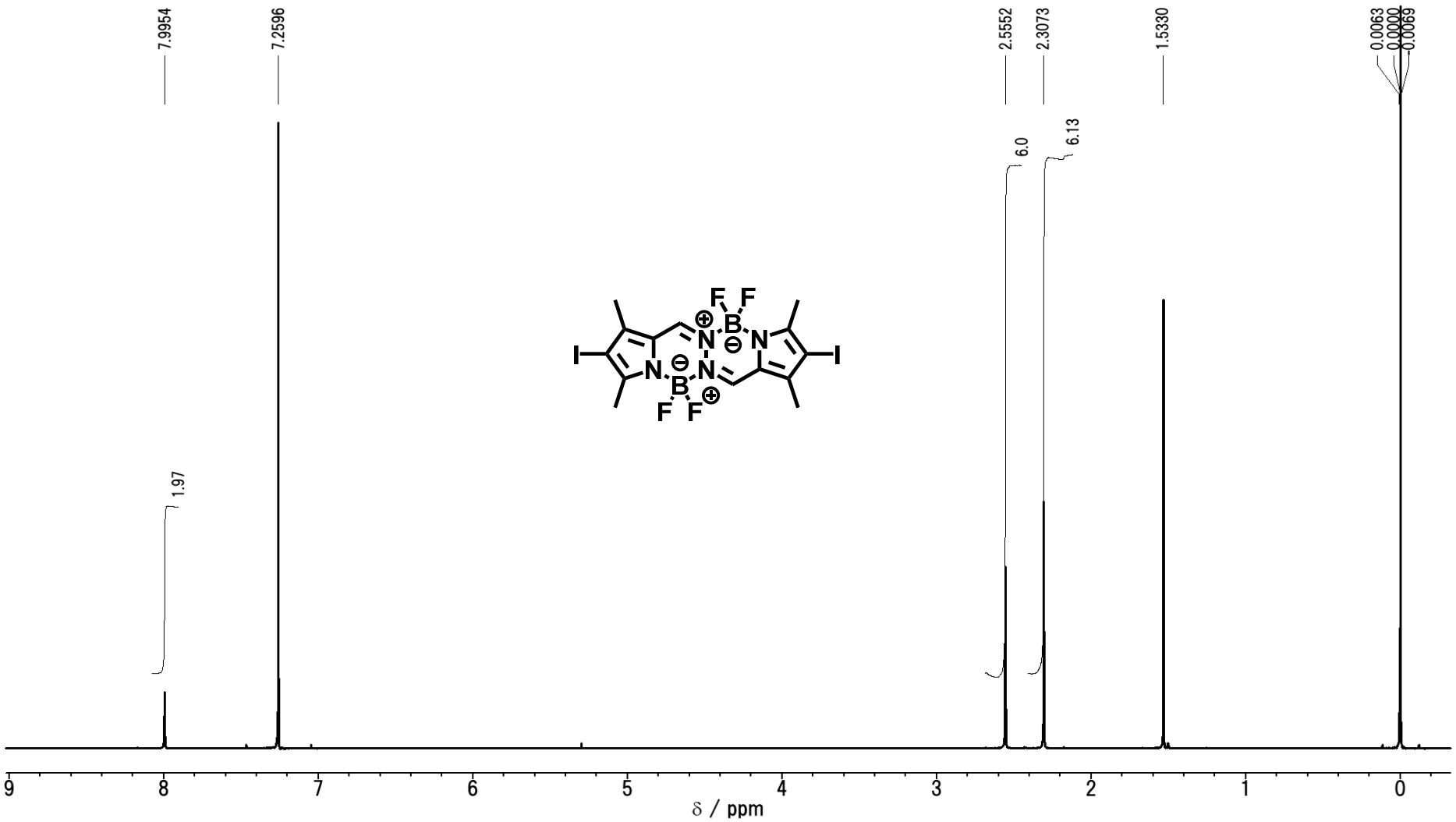

Fig. S23. ^{1}H NMR spectrum of **I_2BOPHY** (500 MHz) in $CDCl_3$.

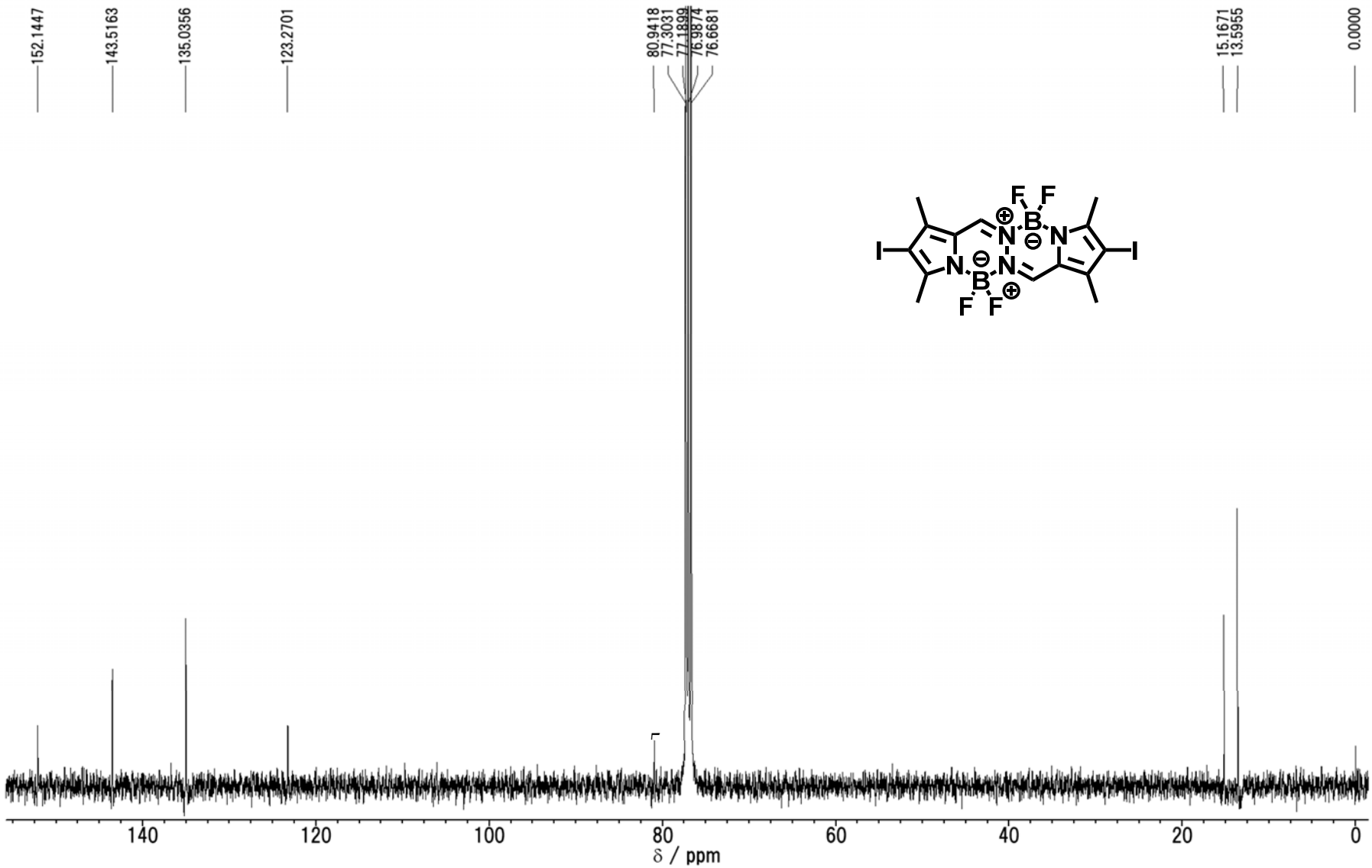

Fig. S24. ^{13}C NMR spectrum of **I$_2$BOPHY** (126 MHz) in $CDCl_3$.

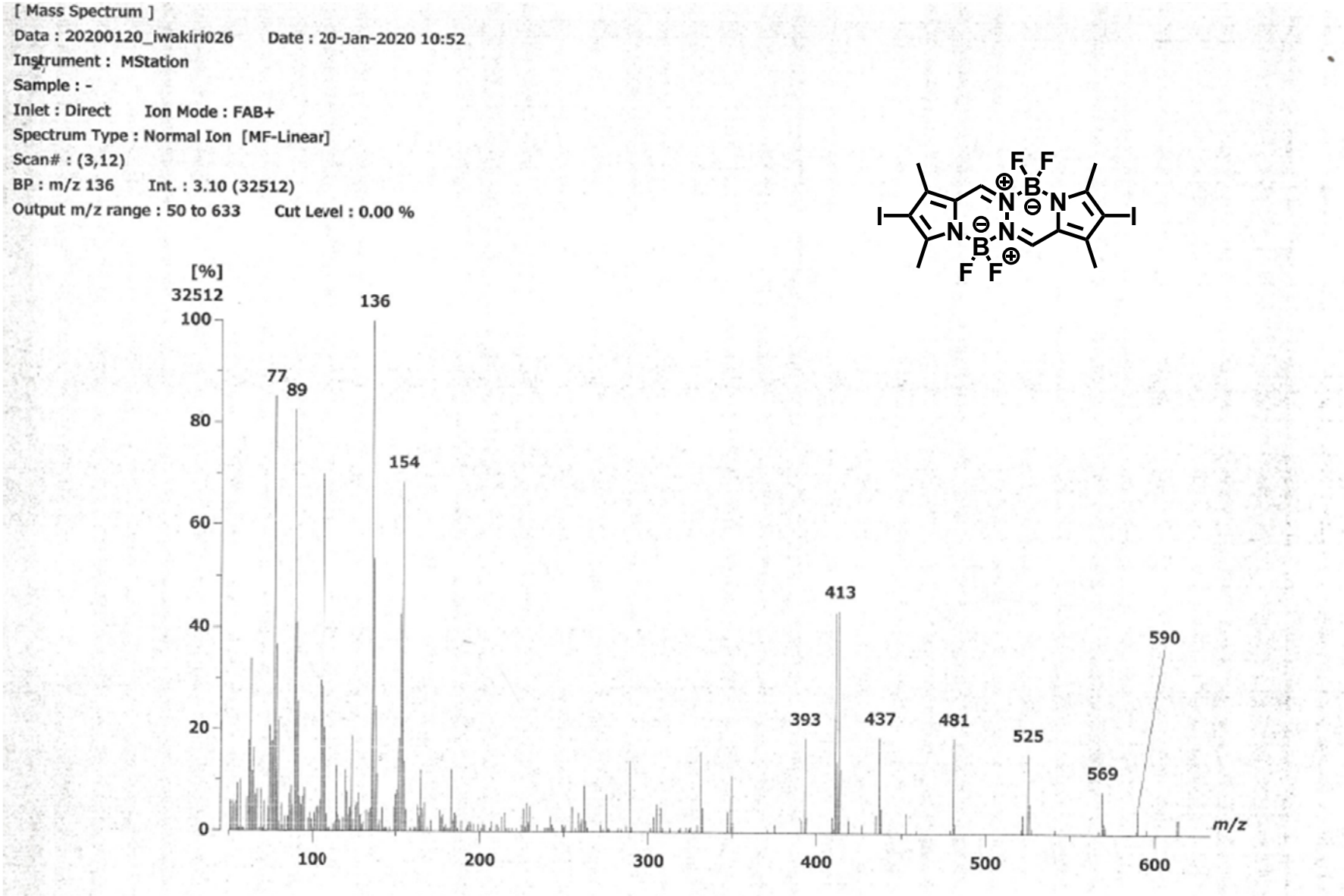

Fig. S25. FAB mass spectrum (positive mode) of **I_2BOPHY.**

Single Crystal Structure Report for **1** (CCDC No. 2057404)

A specimen of $C_{26}H_{24}B_2F_4N_4Se_2$ was used for the X-ray crystallographic analysis. The X-ray intensity data were measured (λ = 1.54178 Å).

The total exposure time was 0.66 hours. The frames were integrated with the Bruker SAINT software package using a narrow-frame algorithm. The integration of the data using a monoclinic unit cell yielded a total of 9290 reflections to a maximum θ angle of 66.54° (0.84 Å resolution), of which 2160 were independent (average redundancy 4.301, completeness = 96.0%, Rint = 3.42%, Rsig = 2.77%) and 2143 (99.21%) were greater than 2σ(F2). The final cell constants of a = 25.0876(11) Å, b = 5.2205(2) Å, c = 22.5474(9) Å, β =120.3860(10)°, volume = 2547.39(18) Å3, are based upon the refinement of the XYZ-centroids of 8291 reflections above 20 σ(I) with 7.059° < 2θ < 133.0°. Data were corrected for absorption effects using the Multi-Scan method (SADABS). The ratio of minimum to maximum apparent transmission was 0.655.

The structure was solved and refined using the Bruker SHELXTL Software Package, using the space group C 1 2/c 1, with Z = 4 for the formula unit, $C_{26}H_{24}B_2F_4N_4Se_2$. The final anisotropic full-matrix least-squares refinement on F2 with 174 variables converged at R1 =2.54%, for the observed data and wR2 = 6.04% for all data. The goodness-of-fit was 1.171. The largest peak in the final difference electron density synthesis was 0.304 $e^-/Å^3$ and the largest hole was -0.320 $e^-/Å^3$ with an RMS deviation of 0.058 $e^-/Å^3$. On the basis of the final model, the calculated density was 1.690 g/cm^3 and F(000), 1288 e^-.

Atom numbering of **1**

Front view

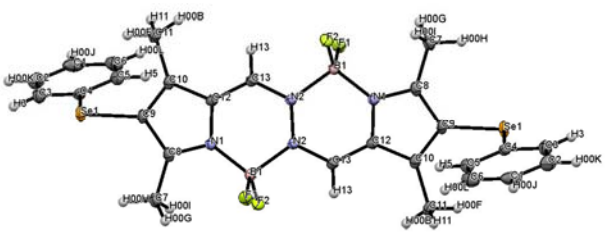

Top view

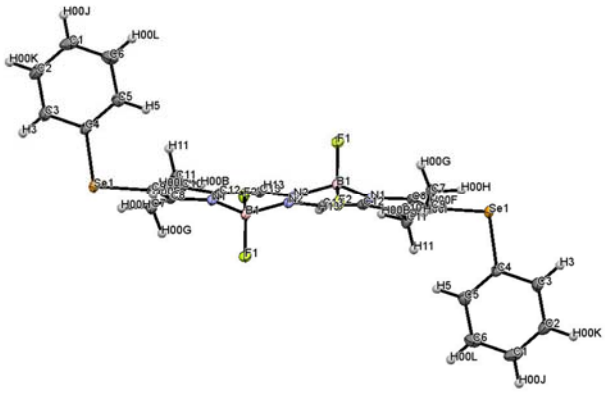

(a)

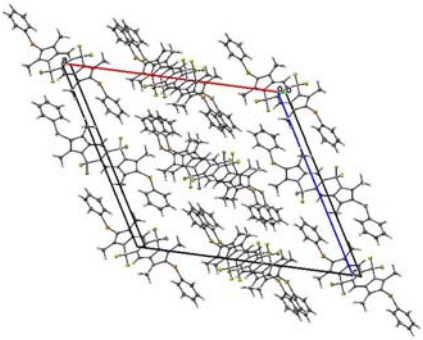

(b)

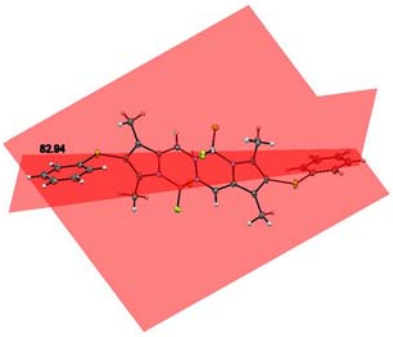

Fig. S26(a) Packing structure, dihedral of BOPHY (b) Dihedral between BOPHY core and phenyl group.

Table S9. Sample and crystal data for **1**.

Identification code	SeBOPHY	
Chemical formula	$C_{26}H_{24}B_2F_4N_4Se_2$	
Formula weight	648.03 g/mol	
Temperature	120(2) K	
Wavelength	1.54178 Å	
Crystal system	monoclinic	
Space group	C 1 2/c 1	
Unit cell dimensions	a = 25.0876(11) Å	α = 90°
	b = 5.2205(2) Å	β = 120.3860(10)°
	c = 22.5474(9) Å	γ = 90°
Volume	2547.39(18) $Å^3$	
Z	4	
Density (calculated)	1.690 g/cm^3	
Absorption coefficient	4.101 mm^{-1}	
F(000)	1288	

Table S10. Data collection and structure refinement for **1**.

Theta range for data collection	4.08 to 66.54°	
Index ranges	-29<=h<=29, -6<=k<=4, -26<=l<=26	
Reflections collected	9290	
Independent reflections	2160 [R(int) = 0.0342]	
Coverage of independent reflections	96.00%	
Absorption correction	Multi-Scan	
Structure solution technique	direct methods	
Structure solution program	SHELXT 2014/5 (Sheldrick, 2014)	
Refinement method	Full-matrix least-squares on F^2	
Refinement program	SHELXL-2018/3 (Sheldrick, 2018)	
Function minimized	$\Sigma\ w(F_o^2 - F_c^2)^2$	
Data / restraints / parameters	2160 / 0 / 174	
Goodness-of-fit on F^2	1.171	
Δ/σ_{max}	0.002	
Final R indices	2143 data; I>2σ(I)	R1 = 0.0254, wR2 = 0.0603
	all data	R1 = 0.0255, wR2 = 0.0604
Weighting scheme	$w=1/[\sigma^2(F_o^2)+5.9672P]$ where $P=(F_o^2+2F_c^2)/3$	
Largest diff. peak and hole	0.304 and -0.320 eÅ^{-3}	
R.M.S. deviation from mean	0.058 eÅ^{-3}	

Table S11. Atomic coordinates and equivalent isotropic atomic displacement parameters (Å^2) for **1**.

	x/a	y/b	z/c	U(eq)
Se1	0.34540(2)	0.74246(4)	0.58820(2)	0.01890(11)
B1	0.40524(10)	0.0629(4)	0.44528(11)	0.0146(4)
F1	0.39062(5)	0.2018(2)	0.38667(6)	0.0206(3)
N1	0.40942(8)	0.2356(3)	0.50176(9)	0.0145(4)
C1	0.33952(11)	0.2730(5)	0.76270(12)	0.0268(5)
N2	0.52701(7)	0.0565(3)	0.52628(8)	0.0139(3)
F2	0.36495(5)	0.8619(2)	0.42973(6)	0.0202(3)
C2	0.30393(10)	0.4892(5)	0.73483(11)	0.0265(5)
C3	0.30583(10)	0.6233(4)	0.68300(11)	0.0223(5)
C4	0.34475(9)	0.5423(4)	0.65935(10)	0.0161(4)
C5	0.38120(9)	0.3257(4)	0.68767(11)	0.0192(4)
C6	0.37813(10)	0.1912(5)	0.73875(11)	0.0250(5)
C10	0.45409(9)	0.5151(4)	0.59194(10)	0.0154(4)
C11	0.50080(10)	0.6657(4)	0.65260(11)	0.0211(4)
C12	0.46563(9)	0.3337(4)	0.55358(10)	0.0142(4)
C13	0.52105(9)	0.2416(4)	0.56227(10)	0.0148(4)
C8	0.36337(9)	0.3525(4)	0.50584(10)	0.0157(4)
C7	0.29711(10)	0.3022(5)	0.45556(11)	0.0214(4)
C9	0.39000(9)	0.5233(4)	0.56207(10)	0.0160(4)

Table S12. Bond length (Å^2) for **1**.

atom	atom	distance	atom	atom	distance
Se1	C9	1.8906(19)	Se1	C4	1.922(2)
B1	F2	1.374(3)	B1	F1	1.384(3)
B1	N1	1.520(3)	B1	N2#1	1.608(3)
N1	C8	1.350(3)	N1	C12	1.396(3)
C1	C2	1.378(4)	C1	C6	1.393(4)
C1	H00J	0.95	N2	C13	1.318(3)
N2	N2#1	1.401(3)	C2	C3	1.384(3)
C2	H00K	0.95	C3	C4	1.394(3)
C3	H3	0.95	C4	C5	1.390(3)
C5	C6	1.384(3)	C5	H5	0.95
C6	H00L	0.95	C10	C9	1.395(3)
C10	C12	1.408(3)	C10	C11	1.497(3)
C11	H00B	0.98	C11	H11	0.98
C11	H00F	0.98	C12	C13	1.388(3)
C13	H13	0.95	C8	C9	1.411(3)
C8	C7	1.487(3)	C7	H00G	0.98
C7	H00H	0.98	C7	H00I	0.98

Table S13. Bond angles (°) for **1**.

C9-Se1-C4	100.80(8)	F2-B1-F1	110.55(16)
F2-B1-N1	113.39(16)	F1-B1-N1	111.23(17)
F2-B1-N2#1	107.36(16)	F1-B1-N2#1	107.45(15)
N1-B1-N2#1	106.54(15)	C8-N1-C12	108.29(17)
C8-N1-B1	128.78(17)	C12-N1-B1	122.09(16)
C2-C1-C6	119.4(2)	C2-C1-H00J	120.3
C6-C1-H00J	120.3	C13-N2-N2#1	117.83(19)
C13-N2-B1#1	117.69(16)	N2#1-N2-B1#1	123.31(19)
C1-C2-C3	120.6(2)	C1-C2-H00K	119.7
C3-C2-H00K	119.7	C2-C3-C4	120.0(2)
C2-C3-H3	120	C4-C3-H3	120
C5-C4-C3	119.76(19)	C5-C4-Se1	122.98(15)
C3-C4-Se1	117.26(16)	C6-C5-C4	119.6(2)
C6-C5-H5	120.2	C4-C5-H5	120.2
C5-C6-C1	120.6(2)	C5-C6-H00L	119.7
C1-C6-H00L	119.7	C9-C10-C12	105.61(17)
C9-C10-C11	127.12(18)	C12-C10-C11	127.26(18)
C10-C11-H00B	109.5	C10-C11-H11	109.5
H00B-C11-H11	109.5	C10-C11-H00F	109.5
H00B-C11-H00F	109.5	H11-C11-H00F	109.5
C13-C12-N1	120.43(18)	C13-C12-C10	130.45(19)
N1-C12-C10	109.05(17)	N2-C13-C12	125.76(19)
N2-C13-H13	117.1	C12-C13-H13	117.1
N1-C8-C9	108.32(17)	N1-C8-C7	122.22(18)
C9-C8-C7	129.43(18)	C8-C7-H00G	109.5
C8-C7-H00H	109.5	H00G-C7-H00H	109.5
C8-C7-H00I	109.5	H00G-C7-H00I	109.5
H00H-C7-H00I	109.5	C10-C9-C8	108.70(17)
C10-C9-Se1	125.98(15)	C8-C9-Se1	125.20(15)

Table S14. Anisotropic atomic displacement parameters (Å^2) for **1**.

	U_{11}	U_{22}	U_{33}	U_{23}	U_{13}	U_{12}
Se1	0.02498(15)	0.01882(15)	0.01945(14)	0.00429(8)	0.01606(11)	0.00988(8)
B1	0.0133(10)	0.0190(11)	0.0124(10)	0.0000(9)	0.0071(9)	0.0018(9)
F1	0.0220(6)	0.0273(7)	0.0137(6)	0.0044(5)	0.0099(5)	0.0080(5)
N1	0.0135(8)	0.0177(9)	0.0125(8)	0.0004(6)	0.0069(7)	0.0028(6)
C1	0.0245(12)	0.0359(13)	0.0167(11)	0.0026(9)	0.0080(9)	-0.0090(9)
N2	0.0115(8)	0.0183(8)	0.0111(7)	-0.0020(6)	0.0051(6)	0.0005(6)
F2	0.0153(6)	0.0225(6)	0.0244(6)	-0.0060(5)	0.0112(5)	-0.0030(5)
C2	0.0252(11)	0.0374(13)	0.0228(11)	-0.0041(10)	0.0165(9)	-0.0039(10)
C3	0.0218(10)	0.0263(12)	0.0220(11)	-0.0004(9)	0.0133(9)	0.0046(9)
C4	0.0159(9)	0.0192(10)	0.0125(9)	-0.0031(8)	0.0069(8)	-0.0010(8)
C5	0.0187(10)	0.0196(10)	0.0189(10)	-0.0008(8)	0.0091(8)	0.0013(8)
C6	0.0232(11)	0.0238(11)	0.0225(11)	0.0049(9)	0.0075(9)	0.0003(9)
C10	0.0196(10)	0.0156(10)	0.0146(9)	0.0022(8)	0.0114(8)	0.0032(8)
C11	0.0230(11)	0.0227(11)	0.0204(10)	-0.0067(9)	0.0130(9)	-0.0002(9)
C12	0.0151(9)	0.0154(10)	0.0122(9)	0.0005(8)	0.0070(8)	0.0006(8)
C13	0.0158(10)	0.0168(10)	0.0126(9)	-0.0005(7)	0.0078(8)	0.0000(7)
C8	0.0172(10)	0.0182(10)	0.0150(9)	0.0039(8)	0.0106(8)	0.0053(8)
C7	0.0166(10)	0.0294(12)	0.0191(10)	-0.0002(9)	0.0097(9)	0.0066(9)
C9	0.0198(10)	0.0184(10)	0.0152(9)	0.0025(8)	0.0127(8)	0.0060(8)

Table S15. Hydrogen atomic coordinates and isotropic atomic displacement parameters (Å^2) for **1**.

	x/a	y/b	z/c	U(eq)
H00J	0.3377	0.1805	0.7979	0.032
H00K	0.2779	0.5467	0.7513	0.032
H3	0.2806	0.7705	0.6635	0.027
H5	0.4081	0.2703	0.672	0.023
H00L	0.4026	0.0418	0.7577	0.03
H00B	0.541	0.6551	0.6554	0.032
H11	0.5043	0.5954	0.6947	0.032
H00F	0.4877	0.8452	0.6475	0.032
H13	0.5579	0.3189	0.5972	0.018
H00G	0.2895	0.3246	0.4088	0.032
H00H	0.2714	0.4224	0.4635	0.032
H00I	0.2868	0.1263	0.4613	0.032